DESIGN OF A GRADED CELLULAR STRUCTURE FOR AN ACETABULAR HIP REPLACEMENT COMPONENT

Hongqing Vincent Wang [a]
R&D Engineer

Scott R. Johnston [b]
Postdoctoral Fellow

David W. Rosen [b]*
Professor

[a] IronCAD Inc., 700 Galleria Parkway, Suite 300, Atlanta, GA 30339
[b] The George W. Woodruff School of Mechanical Engineering, Georgia Institute of Technology Atlanta, GA 30332

* Corresponding Author: 404-894-9668, david.rosen@me.gatech.edu.

Reviewed, accepted September 14, 2006

ABSTRACT

The state-of-the-art porous coatings become more and more popular in uncemented prostheses to make bone grow into implants for biological fixation. In this paper, graded cellular structures are proposed for uncemented prostheses to enhance stability on implant-bone interfaces. As an example study, the authors develop a new acetabular implant with gradient porosity for hip replacement. A gradient porous acetabular component with cellular structure could match the bone's elasticity. Material is adaptively distributed from high porosity at the bone-implant interface to solid metal at the joint's articulating surface. The new acetabular prosthesis would replace metal-on-polyethylene bearing with metal-on-metal bearing for less wear. The design problem of acetabular component is formulated and a requirement list is elaborated. A detailed design of the prosthesis with a graded cellular structure is presented. The design concept is validated with a comparison to the existing products according to the design requirements.

KEY WORDS

Cellular Structure, Unit Truss, Gradient Porosity, Implant-bone Interface, Hip Replacement, Uncemented Prosthesis, Acetabular Implant

1 INTRODUCTION

Joint replacements with prosthesis are becoming more common as the population of the world begins to age. One major issue of prosthesis design is the fixation between the implants (commonly metals) and their surrounding bones. Uncemented prostheses emerged as a new technology to biologically fix implants to bones without the use of cement. Recent clinical results show that uncemented prostheses reduce the aseptic loosening rate and thigh pain in hip replacement [1]. The uncemented prostheses use porous metal surfaces to allow bone ingrowth into the surrounding prostheses as shown in Figure 1 [2, 3]. The uncemented prostheses are coated with multiple layers of micro-porous metal [1, 2] The bone ingrowth into the coating provides additional bonding strength to hold the implant in the desired position.

Researchers have developed various porous coating techniques for biological ingrowth. Typical porous surfaces are plasma sprayed surfaces, sintered beaded surfaces with large spheres, sintered beaded surfaces with small spheres, and diffusion-bonded fiber-metal surfaces [4]. Popular metal coating materials are titanium and tantalum. Common porous coatings have a volume porosity

between 30-70%, with an average pore size ranging between 100 and 1000 μm, and a coating thickness between 500 and 1500 μm [5]. The experimental data shows that a mean pore size $\geq 200 \mu m$ and porosity $\geq 40\%$ are experimentally optimal for bone ingrowth [4].

The current coating techniques provide arguably sufficient bone ingrowth to enhance the implant fixation. The fatigue failure on the implant-bone interface has not been significantly reduced due to a sharp difference among the elastic modulii of the solid metal implant, coating, and bone. The coating porosity and thickness may not be the best for bone ingrowth since most of the implant is solid and has a higher effective density. The porous coating is uniformly applied onto the implant and the thickness cannot exceed 1500 μm. The interconnectivity in the coating is limited because the only currently available coating particle geometries are spheres, beads, and diffused fibers [4].

A graded cellular structure can provide an adaptive and ordered porosity distribution. As displayed in Figure 2, the graded cellular structure gradually can change from thin struts with high porosity and small elasticity on the exterior boundary to thick struts with low porosity and large elasticity on the inner boundary. In this paper, the authors propose to use graded cellular structures in prostheses to enhance joint stability after implantation.

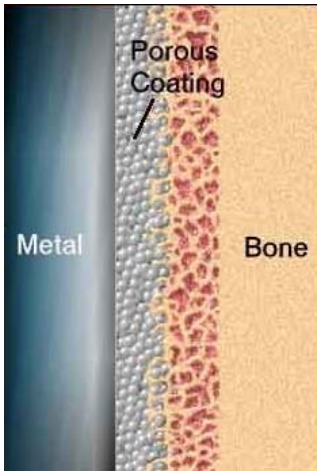

Figure 1. Uncemented metal-bone interface with porous metal coating in prosthesis [1, 2]

Figure 2. An example of cylindrical graded cellular structures (top view)

The bone ingrowth into the porous implant is greatly influenced by the chemical, mechanical and geometric characteristics of the porous coatings in the uncemented prostheses. An elastic modulus matches to the surrounding bone, larger pore spaces, higher porosity and interconnectivity, and improved surface bioactivity can significantly increase bone growth into the gap region and porous coating [6]. The implant with a matching elastic modulus to the bone has less damage on neighboring tissues and a higher fatigue resistance at the bone-implant interface [7]. Higher porosity, higher interconnectivity, and larger pore spaces can improve the surface bioactivity with more breathability to enhance bone ingrowth for stronger prosthesis fixation [4, 8].

The authors present an example of an acetabular component using graded cellular structures for hip replacement. The new prosthesis design can gradually change its elastic modulus, achieve high porosity and pore interconnectivity, and reduce wear rate at the implant-bone interface.

2 DESIGN REQUIREMENTS FOR ACETABULAR COMPONENT IN HIP REPLACEMENT

A conventional acetabular component usually consists of a polyethylene liner and metal shell. In this research, the acetabular component is designed as a single hemispherical part shown in Figure 3 (measurements taken from CAD models supplied by [9]). The measured dimensions of the femoral component, femur and Ilium, the inner and outer radii of the acetabular component are 13.89 mm and 29.50 mm respectively, and the resulting acetabular thickness is 15.61 mm. The gap between the implant and bone must be less than 0.5 mm to allow bone growth into the implant. The total geometric tolerance (resulting from design, manufacturing, and installation) of the hemispheric implant should be no more than 0.5mm, thus the outer radius should be 29.50±0.25 mm. The inner surface as the prosthesis' articulating surface should be very smooth and is usually polished. The interior region of Ilium surrounding the acetabular component is spongy bone with an average elasticity of 1 GPa, and yield strength of 5 MPa. The exterior region of Ilium is compact bone with average elasticity of 16 GPa and yield strength of 175 MPa. The elasticity of the designed acetabular component is desired to gradually change from 1 GPa at its exterior boundary to match the elasticity of Ilium's spongy bone. Before the insertion of acetabular component, the compact bone in the acetabulum area is reamed and the interior spongy bone directly contact the implant [10, 11].

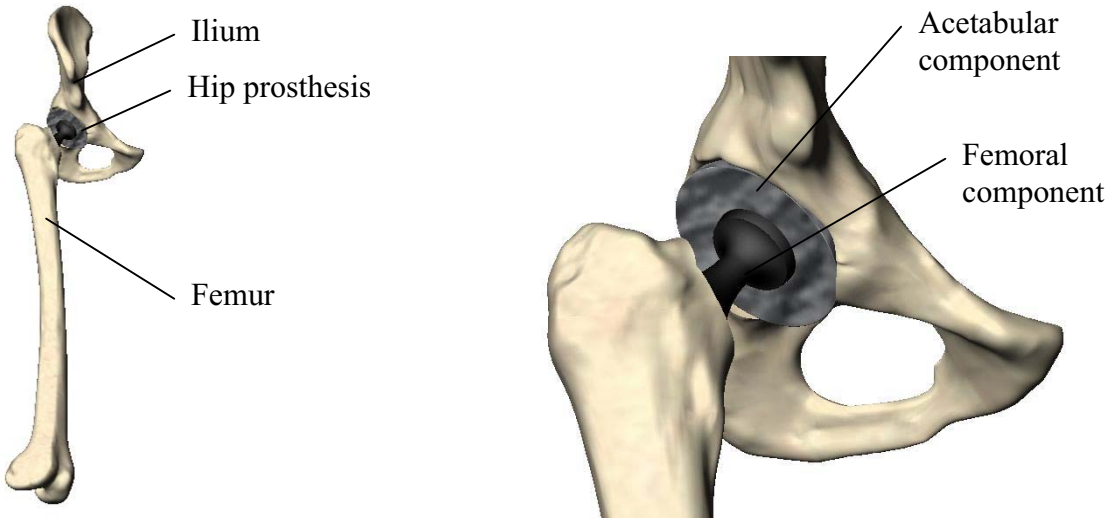

(a) Overall view of in-situ hip prosthesis (b) Close view of in-situ hip prosthesis

Figure 3. New hip prosthesis using a single-piece acetabular component of cellular structure for enhanced stability

In Table-1, the authors elaborate on a design requirement list of an acetabular component for total hip replacement. These requirements represent the design objective, constraints, development demands (D) and wishes (W). The demands are mandatory to satisfy while the wishes should be met to a maximum extent. The objective is to design an acetabular component for better stability than current designs under the design constraints for geometry, material, mechanical and biological properties, manufacturing, and installation.

Table-1. Requirement list of designing acetabular component for enhanced stability

Requirement list for acetabular component of hip replacement		Issued on: 10/11/2005
Problem Statement: Design a acetabular component for enhanced stability	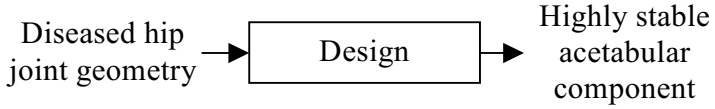	
D/W	Requirements	
	1. Geometry	
D	1.1. Shape fitness (inner radius: 13.89mm; outer radius: 29.50mm; gap between implant and bone $< 0.5mm$)	
D	1.2. Cellular architecture (not discussed in this paper)	
W	1.3. Appropriate porosity ($\geq 40\%$ on implant-bone interface; solid on joint articulating interface)	
D	1.4. Pore size ($\geq 0.2mm$; avoid space collapse and best interconnectivity)	
	2. Mechanical properties	
D	2.1. Comparable elasticity to bone; graded change.	
D	2.2. Adequate strength ($\geq 500MPa$ on articulating surface)	
W	2.3. High fatigue resistance ($\geq 400MPa$ on articulating surface for 10 million cycles)	
W	2.4. Less wear and small debris	
	3. Biological properties	
D	3.1. Biocompatible with bone	
W	3.2. Less or no thrombophlebitis or infection	
	4. Manufacturability	
D	4.1. Manufacturable	
W	4.2. Less delivery time	
W	4.3. Lower cost	
	5. Installation	
W	5.1. Less or no assembly	

3 MATERIAL SELECTION AND MANUFACTURING PROCESS

The first design issue is the material selection for best biocompatibility and sufficient mechanical strength. Biocompatible polymer and ceramic scaffolds (such as polyethylene) have been extensively studied for prosthesis components [12]; however, the mechanical properties of the polymer scaffolds are insufficient to support bone growth under loading conditions, and the ceramic scaffolds are too brittle. A few metal scaffolds, such as titanium and tantalum foam can provide sufficient strength and fatigue resistance because they maintain sufficient mechanical strength and fatigue resistance over extended periods *in vivo* [13]. Porous titanium as well as porous titanium coating have been successful at encouraging bone ingrowth both *in vivo* and in clinical trials [4, 14]. Moreover, titanium possesses excellent biocompatibility with body tissues and is widely used as an implant material. Titanium has excellent fatigue and corrosion resistances. A typical titanium alloy, Ti-6Al-4V, has a yield Strength 900 MPa, ultimate tensile strength 960 MPa, elasticity modulus 110 GPA, and hardness 35 Rc. However, it has a known drawback of its poor resistance to wear, and notch sensitivity when used as bearing material [16]. Tantalum carbide coating is a good candidate for protective hard coatings against wears in sliding applications; therefore, a layer of tantalum carbide coating (780±50nm thick and 53±4% carbon content) may be applied to the articulating surfaces to

reduce the wear [17]. The sliding wear resistance test on a conventional ball-on-disc test apparatus demonstrated that the friction coefficient of tantalum carbide (low carbon) coated surface can be as low as 0.15, which is comparable to the friction coefficient of untreated graphite, 0.14 [18]. In our design, titanium alloy has been selected as the material for cellular structure and solid liner of the acetabular component, and a layer of tantalum carbide will be applied as a coating on the liner's articulating surface.

With the development of additive manufacturing (AM) processes (also known as rapid prototyping), the manufacture of graded cellular structures becomes feasible. AM is capable to manufacture the entire acetabular component as a single part without assembly [19, 20]. AM processes have the potential to manufacture the acetabular component including the porous structure and solid liner section as a single part without assembly as well as with varying architecture, porosity, and pore size of the cellular structure. Selective Laser Melting (SLM) is one of the possible processes to manufacture 3-D porous metallic structures using a variety of material options, including stainless steel, titanium, and chromium-cobalt [21, 22]. SLM resolution is capable of fabricating a strut diameter as small as 0.1mm. The inner surface may be polished to an average roughness of 60nm for better smoothness and coated with a layer of tantalum carbide via vapor deposition [17].

4 MATCHING ELASTIC MODULII WITH GRADED CELLULAR STRUCTURE

A high porosity is required for adequate bone ingrowth into the implant to create adequate fixation to withstand normal physiological loading. Additionally, the implant's mechanical properties should closely match the host's tissue properties at the time of implantation [23, 24]. Since the acetabular component is surrounded by the acetabulum's spongy bone (after implantation), the desired elasticity of exterior layer of cellular structure in the acetabular component should be 1 GPa.

The microstructure of a graded cellular structure can be modeled as a unit truss with a desired elastic modulus value depending upon the truss diameter. An octet unit truss structure has been chosen for this study and two octet trusses with different strut diameters are shown in Figure 4. The elastic modulus of the implanted acetabular component is desired to change gradually from $E_0 = 1.0GPa$ at its boundary, (the Ilium bone) to $E_s = 110GPa$ of the solid titanium. The effective elasticity of the unit truss, E_{eff}, is defined in Equation 1 [25] where L_h denotes the half-strut length and d denotes the strut diameter. To match the desired elasticity at the exterior surface (the Ilium bone), the effective elasticity E_{eff} needs to be as close to $E_0 = 1.0GPa$ as possible. Therefore, using Equation 2, the calculated ratio between the strut diameter and half-strut length is $\frac{d}{L_h} = 0.1241$. The resulting slenderness ratio, $SR = 4\frac{L_h}{d} = 32.2$, is less than the critical slenderness ratio, $SR_{cr} = 34.73$, of a single titanium alloy strut with both ends clamped for the buckling consideration. Hence, yield always occurs earlier than buckling when the cellular structure fails.

(a) $\frac{d}{L_h} = 0.1241,\ SR = 32.2$ (b) $\frac{d}{L_h} = 0.50,\ SR = 8.0$

Figure 4. Graphical representation of a unit truss of the octet truss structure

$$E_{eff} \approx 0.5904 \cdot E_s \left(\frac{d}{L_h} \right)^2 \quad \text{Equation 1}$$

$$\frac{d}{L_h} \approx \sqrt{\frac{E_{eff}}{0.5904 \cdot E_s}} \quad \text{Equation 2}$$

$$SR = \frac{L}{r} = 4\frac{L_h}{d} \quad \text{Equation 3}$$

where,

L – Length of the entire strut

r – Radius of strut cross-section

The lower bound of $\frac{d}{L_h} = 0.1241$ is chosen to match the elasticity of the Ilium bone and the upper bound of $\frac{d}{L_h} = 0.5773$ is set to avoid close-cell in the graded cellular structure as discussed in the next section. The strut diameter linearly changes from $\frac{d}{L_h} = 0.1241$ at the exterior surface of the cellular structure to $\frac{d}{L_h} = 0.5773$ at the interior surface. Hence, the effective elastic modulus of the resulting cellular structure gradually changes from $1.0GPa$ to $21.68GPa$ as shown in Figure 5.

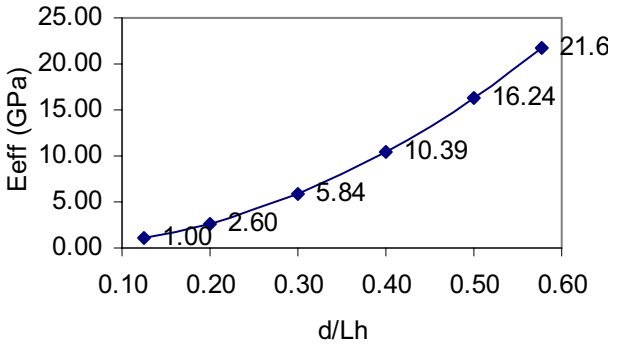

Figure 5. Effective elasticity as a function the ratio of the strut diameter and half-strut length

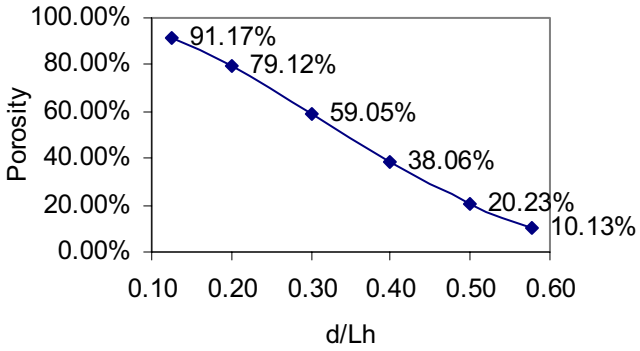

Figure 6. Porosity decreases as diameter increases

5 POROSITY AND PORE SIZE OF GRADED CELLULAR STRUCTURE

A high degree of interconnected porosity can significantly help bone growth into the implant [13]. A porosity of 90% is recommended for optimum diffusive transport within a cell–scaffold construct under *in vitro* conditions [23]. The advantages of scaffold constructed with large surface area to volume ratio has been discussed and demonstrated [24].

The material volume and surface area of the unit trusses with various strut diameters are measured from their solid models. The porosity and surface/volume ratio decreases when the ratio between the strut diameter and strut half-length increase, as displayed in Figure 6. When $\frac{d}{L_h} = 0.1241$, the porosity can reach as high as 91.17% and create a section of the cellular structure having an excellent diffusive transporting capability; conversely, the porosity approaches 0% when $\frac{d}{L_h}$ is approximately 0.65. The strut diameter is restricted by the thickness of the solid section (skin of the cellular structure t_{inner}) to avoid the strut obtrusion from the inner surface of the solid skin section; hence, $\frac{d}{2} \le t_{inner}$ must be satisfied to avoid the strut obtrusion.

For example, when the skin thickness is set as $t_{inner} = 3mm$, the strut diameter must satisfy, $d \le 2t_{inner} = 6mm$. The authors have set $\frac{d}{L_h} = \frac{1}{\sqrt{3}} \approx 0.5773$ for the struts connected to the solid section. When $\frac{d}{L_h} = \frac{1}{\sqrt{3}}$, the cellular structure becomes a close-cell (zero opening, 10.13% porosity), which does not allow for bone ingrowth. Thus, the porosity of the designed graded cellular structure gradually changes from 91.17% to 10.13% (Ilium bone to inner cup). The surface/volume ratio is proportional to the inverse of half strut length, therefore, when evaluating the influence from strut diameter on the surface/volume ratio, the relative surface/volume ratio can be used after multiplying the surface/volume ratio by half the strut length, which avoids using half the strut length parameter. The relative surface/volume ratio gradually decreases from 1.61 at the exterior surface to 0.35 at the inner surface as shown in Figure 7.

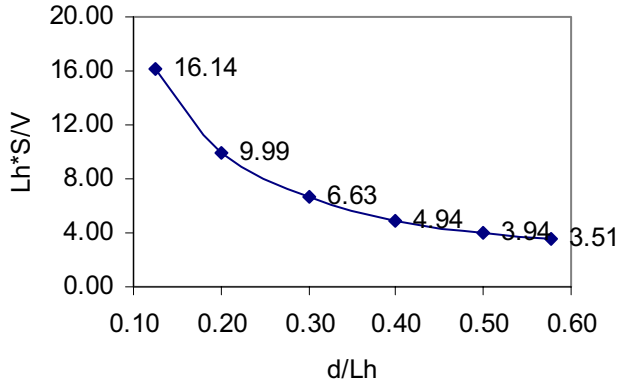

Figure 7. Relative surface/material volume ratio decreases as diameter increases

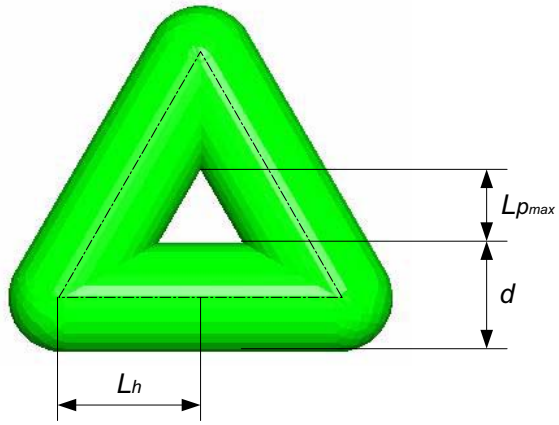

Figure 8. Pore size of octet truss

Brandon has researched various metallic coatings used in hip implants and has determined that the total amount of bone ingrowth does not significantly differ for pore sizes ranging between 200 and 450 μm, but was significantly less for a pore size of 140 μm [4]. Therefore, the optimal pore size for hip implants should be greater than 200 μm. Unfortunately, there is a lacking in literature concerning the maximum allowable pore size.

In our designed graded cellular structure of the acetabular component, the strut diameter starts from 100 μm at the outer surface of the cellular section. Therefore, to exactly match the spongy bone's elasticity $E_0 = 1.0GPa$, the half-strut length L_h should be 805.8 μm as determined by Equation 4.

$$L_h = \frac{d}{0.1241} = \frac{100\mu m}{0.1241} = 805.8\mu m \qquad \text{Equation 4}$$

The designed cellular structure must be open-cell; otherwise, the bone cannot grow into the implant. If the strut diameter increases, the pore size decreases, which results in a closed-cell structure, and is undesirable. The authors provide the largest opening size $L_{p_{\max}}$ of the triangular face of an octet truss (defined in Equation 5 and displayed in Figure 8). The pore size is defined as the average opening size of its triangular face and presented as Equation 6. To ensure a valid open-cell cellular structure for bone ingrowth, the pore size must be larger than zero. Therefore, the strut diameter must satisfy $\frac{d}{L_h} \le \frac{2}{\sqrt{3}} \approx 1.155$ (determined from Equation 6). The pore size can be computed using the strut length and two strut diameters; with $L_h = 805.8\mu m$ and $d = 100\mu m$ ($\frac{d}{L_h} = 0.1241$), the corresponding pore size is $L_p = 622.8\mu m$, and with $L_h = 805.8\mu m$ and $d = 465.2\mu m$ ($\frac{d}{L_h} = 0.5773$), the corresponding pore size is $L_p = 348.9\mu m$.

$$L_{p_{\max}} = \begin{cases} \sqrt{3}L_h - \dfrac{3}{2}d, \text{when } L_h > \dfrac{\sqrt{3}}{2}d \\ 0, \qquad\qquad \text{when } L_h \le \dfrac{\sqrt{3}}{2}d \end{cases}$$ Equation 5

$$L_p = \frac{L_{p_{\max}}}{2} = \begin{cases} \dfrac{\sqrt{3}}{2}L_h - \dfrac{3d}{4}, \text{when } L_h > \dfrac{\sqrt{3}}{2}d \\ 0, \qquad\qquad \text{when } L_h \le \dfrac{\sqrt{3}}{2}d \end{cases}$$ Equation 6

From the above study, the geometric specification for an acetabular component as a graded cellular structure is summarized in Figure 9.

1. Liner section in hemispherical shape 1.1. Outer radius: $R_1 = 16.89mm$ 1.2. Inner radius: $R_2 = 13.89mm$ 2. Cellular section in hemispherical shape 2.1. Outer radius: $R_0 = 29.50mm$ 2.2. Inner radius: $R_1 = 16.89mm$	3. Cellular architecture: octet truss 3.1. Average strut length: $L = 2L_h = 1.611mm$ 3.2. Strut diameter: gradually (linearly) increasing from $d = 100\mu m$ to $d = 465.2\mu m$

Figure 9. Geometric specification of graded cellular structure

The CAD model of the resulting acetabular component (including graded cellular structure and titanium liner) is shown Figure 10 and Figure 11, (there are 79978 struts and 15311 nodes in this cellular structure). The strut diameters change linearly with respect to the distance between the strut and hemisphere center, (increase in strut diameter from exterior to inner surface). The CAD model has been created using a hybrid geometric modeling approach [26].

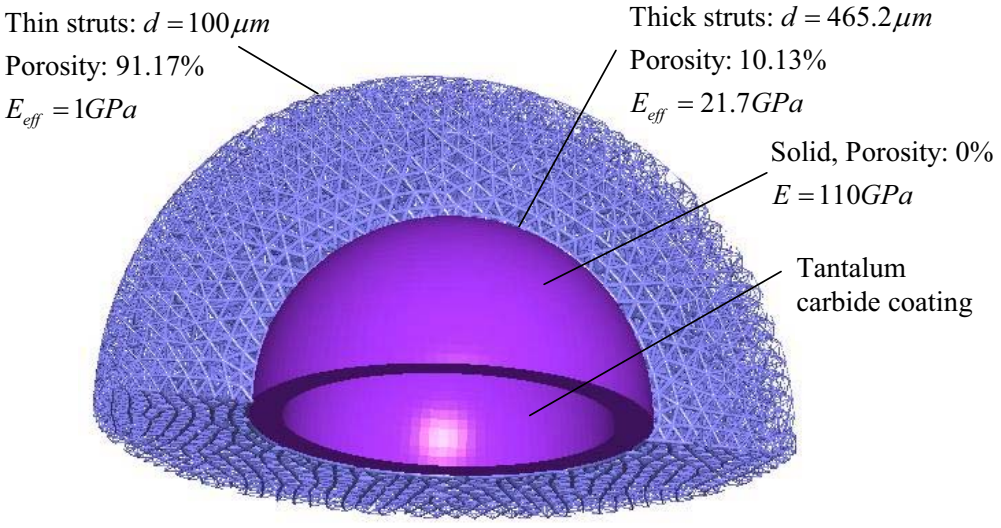

Figure 10. A cross-section view of the STL model of the new acetabular component with graded cellular structure

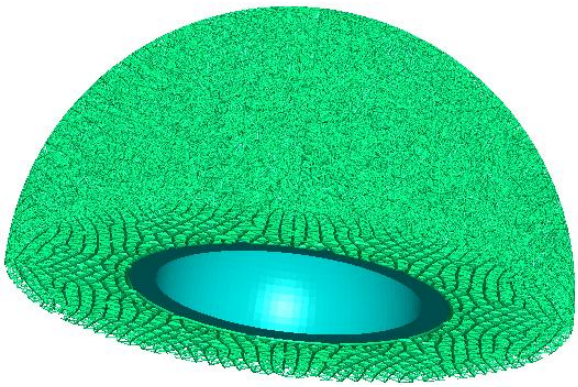

Figure 11. The entire new acetabular component with graded cellular section

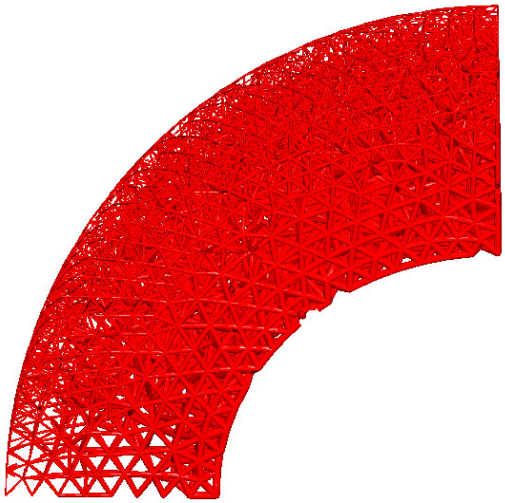

Figure 12. Mechanics analysis using 1/12 of the new acetabular component

6 MECHANICS ANALYSIS OF THE CELLULAR STRUCTURED ACETABULAR COMPONENT AND VALIDATION OF THE CONCEPTUAL DESIGN

The hip joint contact area and pressure distribution during activities of daily living vary from one movement and to another and are relatively complicated. Yoshida has determined that the peak pressure of moderate magnitude is located at the lateral roof of the acetabulum during fast, normal, and slow walking. The peak pressure is located at the edge of the posterior horn during standing up, sitting down, and knee bending motions [27]. The peak pressure varies from 2.87MPa during slow walking to 9.36MPa during sitting down.

For simplicity, the authors have analyzed 1/12 of the acetabular component (shown in Figure 12) and applied a uniform pressure, 9.36MPa, onto the acetabular cup (titanium liner). The external surface is fixed in all 6 degrees of freedom. There are a total of 1255 nodes attached to the inner surface (with an area of $149.4mm^2$) and each node bears an equivalent 1.1N force along the radial direction of the hemispherical cup. The maximum stress among all struts is 23.6MPa with a maximum deflection among all nodes is $0.028mm$. The total strain energy stored in the cellular structure is $0.163N \cdot mm$. The effective elasticity of the cellular section in the radial direction is 3.81 GPa, while the effective elasticity is 1.27 GPa at the outer surface and 23.9 GPa at the inner surface.

The design of new acetabular component is validated through a critical evaluation with the design requirements elaborated in Table-1 and a comparison with current designs is shown in Table-2. A "+" and "-" denote whether the new design is superior to the existing designs, while a "0" denotes no improvement over the current design. All the demand requirements (D) were satisfied and most of wish requirements (W) were accommodated with improved results.

7 CONCLUSIONS

The authors successfully use a graded cellular structure in designing an uncemented acetabular prosthesis for enhanced stability on implant-bone interface. The new design of the acetabular component matches the elasticity of the surrounding bone and gradually changes from high porosity at the implant-bone interface to solid metal at the liner section. Other issues, such as material selection,

manufacturing process, pore sizes, surface/volume ratio have been discussed. The interconnectivity of cellular structure is superior to the porous metal, which are commonly spherical particles or diffused fibers. The elasticity of cellular structure is reconfigurable to match bone's elasticity, while the porous metal is uniform and determined by the manufacturing process and material. The new acetabular component has better fatigue strength and significantly less wear since the metal-on-metal bearing replaces the metal-on-polyethylene bearing. Less assembly is required due to fewer parts.

In order to get closer to transfer this technology to clinical application, several unanswered questions related to implant design must be addressed in the future before a transfer of this technology to clinical trials can be conducted. The architecture type (one of the morphology issue other than porosity and pore size), physical prototyping, part inspection method, and physical experiments for mechanical property analysis have yet to be currently resolved.

Table-2 Critical evaluations on the designed acetabular component

D / W	**Criteria**	**+ /-**	**Comments: comparison with existing acetabular cup with porous coating**
	1. Geometry		
D	1.1. Shape fitness (inner radius: 13.89mm; outer radius: 29.50mm; gap between implant and bone $< 0.5mm$)	-	Gap could be greatly influenced by the manufacturing (e.g. SLM), not as good as existing designs. But it could reach the requirement.
W	1.2. Cellular architecture	+	Type of architecture was not discussed in this research, however capable to provide various architectures. Existing designs have limitation from coating techniques.
W	1.3. Appropriate porosity ($\geq 40\%$ on implant-bone interface; solid on joint articulating interface)	+	90.17% at the implant-bone interface, solid in liner section. Superior to the existing porous coating.
D	1.4. Pore size ($\geq 0.2mm$; avoid space collapse and best interconnectivity)	+	Satisfied: average pore size 1.1mm at the implant-bone interface; good interconnectivity.
	2. Mechanical properties		
D	2.1. Comparable elasticity to bone; gradual change.	+	Satisfied: gradually from $E_0 = 1.0GPa$ to $E_s = 110GPa$
D	2.2. Adequate strength ($\geq 500MPa$ on articulating surface)	0	Satisfied: 900MPa in liner section.
W	2.3. High fatigue resistance ($\geq 400MPa$ on articulating surface for 10 million cycles)	+	700MPa in tantalum carbide coating[28]; 420MPa in solid titanium alloy.
W	2.4. Less wear and small debris	+	Tantalum carbide coating greatly reduces the friction and wear rate. Metal wear debris is in nano-scale.
	3. Biological properties		
D	3.1. Biocompatible with bone	0	Satisfied: perfect biocompatibility between titanium and tissue.
W	3.2. Less or no vein inflammation, infection		Not evaluated yet.
	4. Manufacturability		
D	4.1. Manufacturable	-	Satisfied: minimum manufacturable feature size can be 0.1mm by SLM
W	4.2. Less delivery time	0	A few days.
W	4.3. Lower cost	-	High cost of using rapid prototyping. But acceptable.
	5. Installation		
W	5.1. Less or no assembly	+	The regular polyethylene liner is removed. Less assembly required.

ACKNOWLEDGEMENTS

We gratefully acknowledge the U.S. National Science Foundation, through grants IIS-0120663 and DMI-0522382, and the support of the Georgia Tech Rapid Prototyping and Manufacturing Institute member companies for sponsoring this work.

REFERENCES

[1] M. A. Mont and D. S. Hungerford, "Proximally Coated Ingrowth Prostheses: A Review," *Clinical orthopaedics and related research*, vol. 344, pp. 139-149, 1997.
[2] "A Patient's Guide to Total Hip Replacement Surgery," Medical Multimedia Group http://www.healthpages.org/AHP/LIBRARY/HLTHTOP/THR/INDEX.HTM, October 16, 2005
[3] "Hip Replacement," Biomet, Inc. http://www.biomet.com/patients/hip_replacement.cfm, October 16, 2005
[4] C. R. Bragdon, M. Jasty, M. Greene, H. E. Rubash, and W. H. Harris, "Biologic Fixation of Total Hip Implants," *Journal of Bone & Joint Surgery*, vol. 86, pp. 105-117, 2004.
[5] "*Code of Federal Food and Drug Administration Regulations: Hip joint metal/polymer/metal semi-constrained porous-coated uncemented prosthesis*," Wikipedia, Rockville MD, 2006.
[6] M. Jasty, C. Bragdon, D. Burke, D. O'Connor, J. Lowenstein, and W. Harris, "In vivo skeletal responses to porous-surfaced implants subjected to small induced motions.," *Journal of bone and joint surgery*, vol. 79, pp. 707-714, 1997.
[7] S. Suresh, "Graded Materials for Resistance to Contact Deformation and Damage," *Science*, vol. 292, pp. 2447-2451, 2001.
[8] Nancy Elftman, "Orthotic Materials: Cellular urethanes combine durability with breathability," in *BioMechanics*, 1998.
[9] M. Viceconti, "Visible Human Male - Bone surfaces," Laboratorio di Tecnologia Medica, Istituti Ortopedici Rizzoli http://www.tecno.ior.it/VRLAB/researchers/repository/BEL_repository.html, October 01, 2005
[10] W. Sun, B. Starly, J. Nam, and A. Darling, "Bio-CAD modeling and its applications in computer-aided tissue engineering," *Computer-Aided Design*, vol. 37, pp. 1097–1114, 2005.
[11] A. Maciel, "*Biomechanics of Hip Joint Capsule*," Computer Graphics Lab, Institute of Computing and Multimedia Systems, School of Computer and Communication Sciences, Swiss Federal Institute of Technology, March 30, 2002, 2002.
[12] T. Albrektsson and C. Johansson, "Osteoinduction, osteoconduction and osseointegration," *European Spine Journal*, vol. 10, pp. 96-101, 2001.
[13] J.-P. St-Pierre, M. Gauthier, L.-P. Lefebvre, and M. Tabrizian, "Three-dimensional growth of differentiating MC3T3-E1 pre-osteoblasts on porous titanium scaffolds," *Biomaterials*, vol. 26, pp. 7319-7328, 2005.
[14] Z. LD, P. DE, D. LD, M. DW, N. LA, and P. R., "Structure, metallurgy, and mechanical properties of a porous tantalum foam," *Journal of Biomedical Materials Research*, vol. 58, pp. 180-187, 2001.
[15] H. Uhthoff, D. Bardos, and M. Liskova-Kiar, "The advantages of titanium alloy over stainless steel plates for the internal fixation of fractures: an experimental study in dogs," *The Journal of Bone and Joint Surgery*, vol. 63, pp. 427-434, 1981.
[16] H. Agins, N. Alcock, M. Bansal, E. Salvati, P. Wilson, P. Pellicci, and P. Bullough, "Metallic wear in failed titanium-alloy total hip replacements. A histological and quantitative analysis," *The Journal of Bone and Joint Surgery*, vol. 70, pp. 347-356, 1988.
[17] E. Martinez, U. Wiklund, J. Esteve, F. Montala, and L. L. Carreras, "Tribological performance of TiN supported molybdenum and tantalum carbide coatings in abrasion and sliding contact," *Wear*, vol. 253, pp. 1182–1187, 2002.
[18] H. Kita, M. Fukushima, D. D. Jayaseelan, Y.-P. Zeng, and K. Ohsumi, "Oxidation Resistance and High-Temperature Lubricating Properties of Magnesium-Phosphate-Treated Graphite," *Journal of the American Ceramic Society*, vol. 88, pp. 2632-2634, 2005.

[19] H. Wang and D. W. Rosen, "Computer-aided design methods for additive fabrication of truss structures," International Conference on Manufacturing Automation (ICMA2002), Hong Kong, China, pp. 181-198, December, 2002
[20] P. Jacobs, *Rapid prototyping & manufacturing: fundamentals of stereolithography*, 1st ed, SME, Dearborn, MI, 1992.
[21] J.-P. Kruth, P. Mercelis, J. V. Vaerenbergh, L. Froyen, and M. Rombouts, "Binding mechanisms in selective laser sintering and selective laser melting," *Rapid Prototyping Journal*, vol. 11, pp. 26-36, 2005.
[22] "A NEW world-class generative process developed for direct product realisation with SELECTIVE LASER MELTING (SLM)," MCP Group http://www.mcp-group.com/rpt/rpttslm.html, October 15, 2005
[23] D. W. Hutmacher, "Scaffolds in tissue engineering bone and cartilage," *Biomaterials*, vol. 21, pp. 2529-2543, 2000.
[24] D. W. Hutmacher, "Scaffold design and fabrication technologies for engineering tissues — state of the art and future perspectives," *Journal of Biomaterials Science -- Polymer Edition*, vol. 12, pp. 107-124, 2001.
[25] H. Wang, "*A unit cell approach for lightweight structure and compliant mechanism*," PhD Dissertation, School of Mechanical Engineering, Georgia Institute Of Technology, Atlanta, GA, 2005.
[26] H. Wang, Y. Chen, and D. W. Rosen, "A Hybrid Geometric Modeling Method For Large Scale Conformal Cellular Structures," ASME Computers and Information in Engineering Conference, Long Beach, California, September 24-28, 2005, 2005, Paper Number: DETC02/CIE-34495
[27] H. Yoshida, A. Faust, J. Wilckens, M. Kitagawa, J. Fetto, and E. Y.-S. Chao, "Three-dimensional dynamic hip contact area and pressure distribution during activities of daily living," *Journal of Biomechanics*, vol. 39, 2006.
[28] M. Niinomi, "Fatigue performance and cyto-toxicity of low rigidity titanium alloy, Ti-29Nb-13Ta-4.6Zr," *Biomaterials*, vol. 24, pp. 2673-2683, 2003.